Research in Astron. Astrophys. **2009** Vol. **9** No. **8**, 901 – 910
http://www.raa-journal.org *http://www.iop.org/journals/raa*

Research in Astronomy and Astrophysics

A truncated accretion disk in the galactic black hole candidate source H1743–322

Kandulapati Sriram[1], Vivek Kumar Agrawal[2,3] and Arikkala Raghurama Rao[2]

[1] Department of Astronomy, Osmania University, Hyderabad 500007, India; *astrosriram@yahoo.co.in*
[2] Department of Astronomy and Astrophysics, Tata Institute of Fundamental Research, Mumbai 400005, India
[3] Indian Space Research Organization, New BEL Road, Bangalore 560094, India

Received 2009 February 2; accepted 2009 April 10

Abstract To investigate the geometry of the accretion disk in the source H1743–322, we have carried out a detailed X-ray temporal and spectral study using RXTE pointed observations. We have selected all data pertaining to the Steep Power Law (SPL) state during the 2003 outburst of this source. We find anti-correlated hard X-ray lags in three of the observations and the changes in the spectral and timing parameters (like the QPO frequency) confirm the idea of a truncated accretion disk in this source. Compiling data from similar observations of other sources, we find a correlation between the fractional change in the QPO frequency and the observed delay. We suggest that these observations indicate a definite size scale in the inner accretion disk (the radius of the truncated disk) and we explain the observed correlation using various disk parameters like Compton cooling time scale, viscous time scale etc..

Key words: accretion, accretion disk — binaries: close — stars: individual (H1743–322) — X-rays: binaries

1 INTRODUCTION

The geometry of the inner accretion disk in Galactic Black Hole Candidates (GBHCs) is still a matter of debate. All GBHCs show distinct patterns of temporal and spectral characteristics in different spectral states, most probably due to the geometric configurations attained by the disk in each of the spectral states (Esin et al. 1997). Simultaneous spectral and temporal studies during the X-ray outburst of GBHCs may give a clearer idea about the nature of the disk, because the sources show state transitions during such episodes. Recently, several black hole sources were studied during their outburst period and all of them show a similar trend in their spectro-temporal evolution (Kalemci et al. 2006; Remillard & McClintock 2006; Belloni et al. 2005; Tomsick et al. 2005; Rodriguez et al. 2004). The typical broad band X-ray spectrum of a GBHC shows two primary components, a soft component (from the disk) and a hard component from the Comptonization process (Shapiro et al. 1976; Sunyaev & Titarchuk 1980) or from the base of the jet (Markoff et al. 2005).

One of the important spectral states in GBHCs is the Very High State (VHS) or the Steep Power-law State (SPL) (McClintock & Remillard 2004). Many of the black hole systems become bright during this state and show the 'C' type Quasi Periodic Oscillations (QPOs with high coherence and which are accompanied by flat top noise) and occasionally high frequency QPOs in their Power Density Spectrum (PDS) (Remillard & McClintock 2006). Jets are the most common phenomena in GBHCs and the study of hardness-intensity diagrams (HIDs) shows that the jet switches on/off during this state (Fender et al. 2004). The observational results suggest that the hard component in the SPL state arises due to Comptonization of soft photons originating from a Keplerian disk (Kubota & Makishima 2004; Done & Kubota 2006) and it was found that the disk is truncated, favoring a disk+quasi-spherical cloud geometry (Zdziarski et al. 2002). A detailed justification for assuming the truncated accretion disk scenario, particularly in the SPL state, is given in Done et al. (2007).

The cross-correlation between soft and hard X-ray emission gives further insight into the truncated disk scenario. Three sources, viz. Cyg X-3, GRS 1915+105 and XTE J1554–564, showed anti-correlated hard lags between soft and hard photons in the time scale of a few hundred to a few thousand seconds (Choudhury & Rao 2004; Choudhury et al. 2005; Sriram et al. 2007). XTE J1550–564 and GRS 1915+105 (both sources were in the SPL state) showed model independent and dependent spectral changes along with shifts in the QPO centroid frequencies. The changes in the QPO centroid frequencies were well correlated with the soft as well as hard X-ray fluxes. Recently, similar kinds of time lags were observed in Cyg X-2, a neutron star binary system (Lei et al. 2008). The observed anti-correlated hard lag was attributed to the viscous time scale during which the truncated disk makes radial inward/outward movements. Since XTE J1550–564 and H1743–322 show similar spectral and temporal variability characteristics (McClintock et al. 2007), we have searched for the anti-correlated hard lags between soft and hard X-ray photons in the source H1743–322. The purpose of searching for an anti-correlated hard lag in H1743–322 is to strengthen the idea of the truncated disk scenario in the SPL state.

Despite the lack of dynamical confirmation of the mass of the compact object in H1743–322, it is believed to be a black hole source due to its spectro-temporal characteristics (Corbel et al. 2006; Kalemci et al. 2006; McClintock & Remillard 2004). H1743–322 was discovered with the *Ariel V* all sky monitor in 1977 (Kaluzienski & Holt 1977) and was precisely located by HEAO-I (Doxsey et al. 1977). The 2003 outburst of the source was observed in various wavelengths from X-ray by INTEGRAL (Revnivtsev et al. 2003) and RXTE (Markwardt & Swank 2003), infrared (Baba et al. 2003), optical (Steeghs et al. 2003), to radio (Rupen et al. 2003). The source showed relativistic jet emission (Rupen et al. 2004) similar to GRS 1915+105 and XTE J1550–564. During the 2003 outburst, H1743–322 was in SPL and Thermal Dominated (TD) states for most of the time and it was occasionally in the Hard State (McClintock et al. 2007).

In this paper, we have selected all the SPL states during the 2003 outburst (McClintock et al. 2007) and searched for the anti-correlated hard lags between soft (2–5 keV) and hard (20–50 keV) X-ray bands. In three observations, we have found lags between soft and hard X-ray emission and for two observations, we found a shift in the QPO centroid frequency. We have also found pivoting and marginal pivoting patterns in the spectra, similar to Cyg X-3, GRS 1915+105 and XTE J1550–564. Detailed spectral studies have been carried out to understand the disk-corona configuration in the SPL state.

2 ANALYSIS AND RESULTS

We have used *Rossi X-ray Timing Explorer* (RXTE) observations to study the temporal and spectral behavior of the source H1743–322 and have used the data from the Proportional Counter Array (PCA) (Jahoda et al. 2006) and the High-Energy X-ray Timing Experiment (HEXTE) (Rothschild et al. 1995), effectively covering the 2–150 keV energy band. H1743–322 showed an outburst in 2003 and extensive observations were carried out using the RXTE satellite. Detailed spectral and temporal studies have been carried out and all the observations were classified as SPL, TD and Hard spectral states (McClintock et al. 2007). We have chosen all the SPL states to look for the anti-correlated hard lags. We have used Standard 2 data to obtain the light curves and spectra and followed all the procedures for data filtering and background corrections. For light curves, data were obtained from all the PCUs which were ON (it was noticed that most of the time PCU0 and PCU2 were ON). For obtaining spectra, PCU2 was chosen since it is the most well calibrated among all the PCUs. A 0.5% systematic error is applied to the PCA spectra. We have taken the data from the single bit mode to obtain the Power Density Spectra (PDS) for the observations where the lag was observed. To obtain the 20–150 keV spectra, we have used the HEXTE cluster A data and applied all the necessary corrections. We have used HEASOFT 6.2 soft-

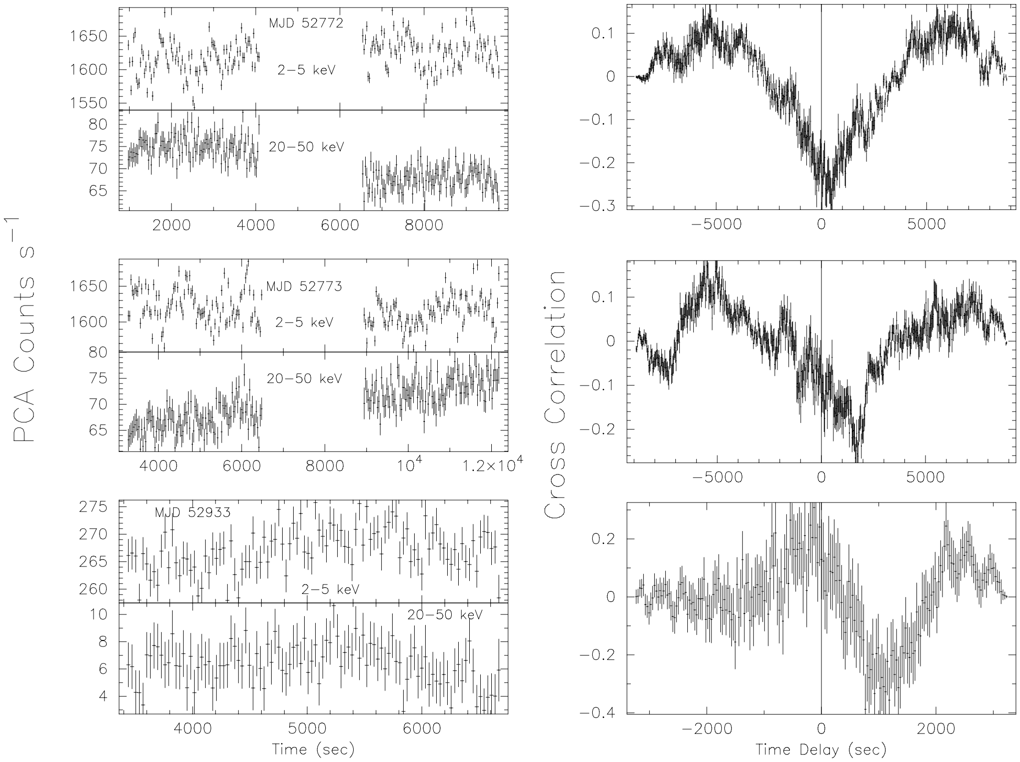

Fig. 1 Soft and hard X-ray band light curves along with the respective cross correlation plots. *Left panels*: soft and hard X-ray band lightcurves, *Right panels*: corresponding cross-correlations of soft and hard light curves. The vertical line at zero is drawn for clarity.

ware to reduce the data and XSPEC 11.3.1 for spectral analysis. All the errors mentioned throughout the paper are of nominal 90% confidence level ($\Delta\chi^2 = 2.7$).

For all the SPL state observations, we have extracted the light curves in two different energy bands. The first energy band spans 2–5 keV (soft) and the second one spans 20–50 keV (hard). The basic idea of dividing the light curves into two bands is that the soft band covers most of the soft photons originating from the Keplerian disk and the hard band covers most of the hard photons coming from the Comptonization region in the accretion disk. We have used the *crosscor* program provided by Ftools. For more details see Sriram et al. (2007). Out of 170 observations, 90 were in the SPL state and anti-correlated hard lags were found in three observations. The observed light curves in the two energy bands are shown in Figure 1, along with the cross-correlation plots. The last observation is quite soft (with the 20–50 keV count rates of only about 6 s^{-1} compared to the 60–80 s^{-1} in the other two observations) and we note that there were no type 'C' QPOs during this observation. This particular observation is found to be in the Hard SPL state (McClintock et al. 2007). We have used the method given in Sriram et al. (2007) to measure the lags and the errors in them and these are given in Table 1. The detected lags range from a few 100 s to 1000 s, similar to what was found in XTE J1550–564 and GRS 1915+105.

To study the variation of the source properties during the periods of the observed lags, we have made a detailed analysis of the initial (Part A) and final (Part B) observations, each lasting for 300 s. Examination of the model independent spectra showed that there were minute changes indicating pivoting and marginal pivoting. Similar kinds of pivoting features were observed in Cyg X-3, XTE J1550–564 and GRS 1915+105 (Choudhury & Rao 2004; Choudhury et al. 2005; Sriram et al. 2007). In the first and the second observations, there is a sharp pivoting around $\sim$6.0 keV whereas no

Table 1 Details of the Observed Anti-correlated Hard Lags

ObsID	Delay (s)	bin (s)	Correlation Coefficient
80146–01–36–00	442.16 ± 37.5	32	-0.30 ± 0.04
80146–01–37–00	1590.65 ± 57.5	32	-0.33 ± 0.04
80137–01–22–00	1129.74 ± 42.0	32	-0.39 ± 0.12

Table 2 Details of the spectral and temporal parameters in individual parts of the respective observations. A and B correspond to the initial and final parts of the observation.

Parameters	80146–01–36–00		80146–01–37–00		80137–01–22–00	
	A	B	A	B	A	B
$kT_{\rm in}{}^a$	0.32 ± 0.01	0.28 ± 0.01	0.28 ± 0.01	0.29 ± 0.01	0.66 ± 0.02	0.63 ± 0.02
$\Gamma_{\rm th}{}^b$	2.07 ± 0.01	2.05 ± 0.01	2.12 ± 0.01	2.10 ± 0.01		
$kT_{\rm e}{}^c$	8.23 ± 0.33	6.94 ± 0.28	9.44 ± 0.91	8.95 ± 0.90		
$N_{\rm th}{}^d$	0.74 ± 0.01	0.75 ± 0.26	1.04 ± 0.20	0.85 ± 0.24		
$\Gamma_{\rm Pl}{}^e$	-	-	-	-	2.13 ± 0.09	2.37 ± 0.09
$N_{\rm Pl}{}^f$	-	-	-	-	0.31 ± 0.01	0.57 ± 0.12
χ^2/dof	117/80	104/80	83/82	114/82	72/84	76.28/84
disk flux^g	61.40	120.56	119.01	84.26	4.32	3.96
thcomp flux	10.11	8.65	12.67	11.30	-	-
Powerlaw flux	10.54	15.32	8.98	13.94	3.96	5.60
Simultaneous fit						
$N_{\rm th}$	0.84 ± 0.04	0.47 ± 0.05	1.07 ± 0.22	0.94 ± 0.22		
$N_{\rm bb}/1000$	504 ± 31	444 ± 27	917 ± 176	587 ± 108		
$kT_{\rm in}$	0.30(fix)	0.30(fix)	0.28(fix)	0.28(fix)		
$\Delta N_{\rm th}/N_{\rm th}(\%)$	44	-	12	-		
$\Delta N_{\rm bb}/N_{\rm bb}(\%)$	12.0	-	36			
Delay (s)	442.16 ± 37.5	-	1590.65 ± 57.5	-	1129 ± 42.0	-
ν (Hz)^h	1.78 ± 0.02	1.87 ± 0.02	2.02 ± 0.02	1.86 ± 0.02		
$\Delta\nu/\nu$ %	5.00	-	-7.92	-		

^{a} Disk Temperature using diskbb model;
^{b} *thcomp* index;
^{c} Electron Temperature;
^{d} *thcomp* normalization;
^{e} Powerlaw index;
^{f} Powerlaw normalization;
^{g} The flux unit for all the models is 10^{-9} erg cm^{-2} s^{-1};
^{h} QPO centroid frequency.

pivoting feature is observed in the third observation. It should be noted that during all the observations of the lags, the sources were in the SPL/VHS spectral state and the study of different GBHCs suggests that the thermal Comptonization process is the working mechanism in this state (Done & Kubota 2006; Kubota & Makishima 2004; Zdziarski et al. 2004).

We have carried out a detailed spectral analysis to uncover and constrain the spectral parameters responsible for the anti-correlated hard lags. We have obtained the spectra covering 2.5–150 keV from the initial and final part of the light curves and fit the data using the multi-component model *diskbb+thcomp+Power-law*. The *diskbb model* (Makishima et al. 1986) takes care of the soft part of the spectrum, *thcomp* (thermal Comptonization model) (Zdziarski et al. 1996) handles the hard spectrum produced by this process and the Power-law model represents the high-energy non-thermal photons. Edges and a Gaussian line near 6.4 keV were used whenever the residuals indicated their presence. Four components were frozen: hydrogen column density $N_{\rm H}$= 2.2 × 10^{22} cm^{-2}, Gaussian line energy

$E = 6.4$ keV and line width = 0.2 keV and the Power-law index $\Gamma = 2.2$. We have verified that keeping these parameters free does not change the results appreciably. The derived spectral parameters are shown in Table 2.

In the first and the second observations, the disk temperature is found to be very low - $kT_{\rm in}$~0.30 keV (see Table 2). There is a notable change in the electron temperature in the second observation. The third observation does not require the *thcomp* model, particularly because of the low count rates in the hard X-ray band. We have used the diskbb+Power-law model for this observation and the Power-law index has steepened from $\Gamma \sim$2.13 to $\Gamma \sim$2.37 whereas the difference in the disk temperature is less contrasting.

To know which parameters are responsible for the model independent pivoting, we have fitted the respective spectra of an observation simultaneously. We have followed the same procedure as used in our earlier work (Sriram et al. 2007).

We found that in the first and the second observations, the normalizations of the disk and the *thcomp* components have changed during the two different parts of the respective observations and it seems that this change is responsible for the observed lag and pivoting (see Table 2). We have not carried out this method for the third observation because of the low count rates at high energies.

We have calculated the unabsorbed disk and *thcomp* fluxes (see Table 2) for the three observations. In the first observation, the disk and *thcomp* fluxes are anti-correlated whereas in the second observation a similar anti-correlation is noticed if we also include the Power-law flux. In the last observation, the disk and Power-law fluxes are anti-correlated (see Table 2). Similar kinds of results were observed in the case of XTE J1550–564 and GRS 1915+105, giving more credence to the truncated accretion disk geometry found from the SPL spectra in these three black hole sources.

2.1 Quasi-Periodic Oscillations

H1743–322 shows all kinds of QPOs ranging from LFQPOs (Low Frequency Quasi Periodic Oscillations) to HFQPOs (Homan et al. 2005; Remillard et al. 2006; McClintock et al. 2007). The origin of HFQPOs is unknown and the production of these features may be due to some resonance mechanisms (Abramowicz & Kluzniak 2001), whereas LFQPOs generally mimic the Comptonization region in the accretion disk (Chakrabarti & Manickam 2000; Titarchuk & Fiorito 2004). During the anti-correlated hard lag, the QPO centroid frequency changes in GRS 1915+105 and XTE J1550-564 (Choudhury et al. 2005; Sriram et al. 2007). We have used single bit mode data (SB_125us_8-13_1s) to obtain the respective PDS (Power Density Spectrum) of the initial and final parts of the observations in which lags were detected. In two observations, QPO features were observed (see Table 2) and they are modeled by a Lorentzian function along with a power law to the continuum. We found that the QPO centroid frequency is shifted towards either low or high frequency (see Fig. 2). The last observation (ObsID 80137–01–22–00) does not have a QPO in its PDS. The relative shift of the QPO centroid frequency between two parts of the observations suggests a change in the geometrical/physical aspect of the Comptonizing region during the detected lags.

3 DISCUSSION AND CONCLUSIONS

The detailed study of the sources GRS 1915+105 and XTE J1550-564 shows that during the observed lags, the spectral as well as the temporal properties significantly change, favoring a truncated disk scenario. Both sources show a pivoting feature and changes in the spectral parameters during the lags (Choudhury et al. 2005; Sriram et al. 2007). The lags obtained between soft and hard flux in SPL/VHS state clearly suggest that the changes in accretion disk structure may be because of relative changes in the mass accretion rate. The model independent spectra show that during the lag, the spectra change and show a pivoting pattern. The pivoting in the spectra directly gives an idea of change in the flux in softer and harder parts of the spectra. The detected lags most likely indicate the viscous time scale during which the disk front moves inward/outward depending on the local mass accretion rate and hence the soft and hard emission regions change their respective temporal and spectral properties.

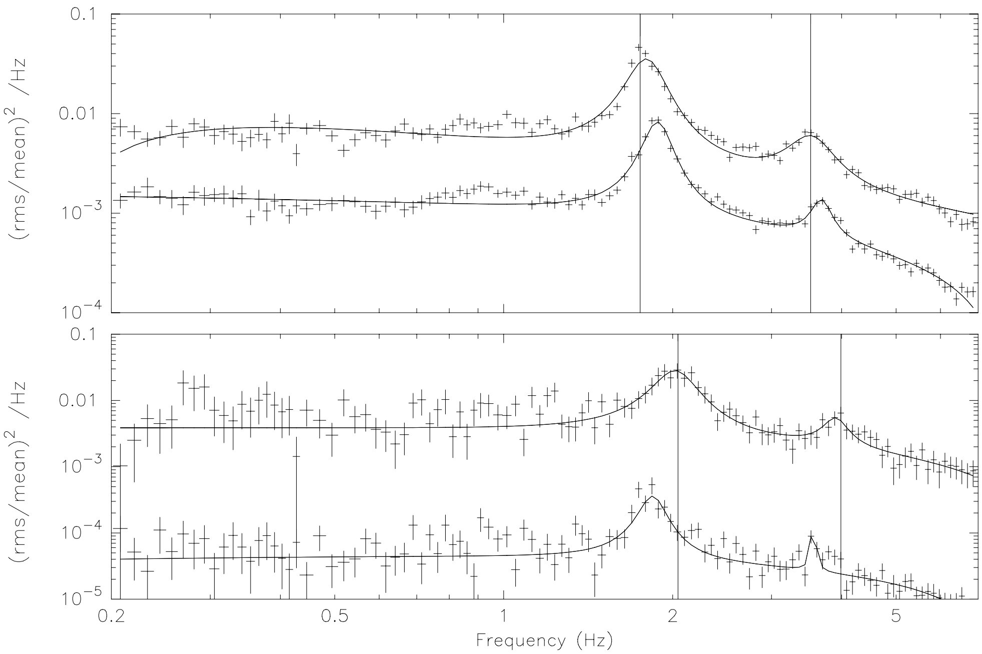

Fig. 2 Change in the centroid frequency in the initial and final parts (parts A and B) of the light curve ObsID 80146–01–36–00 (*top panel*) and ObsID 80146–01–37–00 (*bottom panel*). The lines are drawn to mark the shift and the part B data is shifted vertically for clarity.

From the spectral analysis of the first observation, we found that the disk temperature is not changing but the electron temperature of the Compton cloud changes ($\delta kT_{\rm e} \sim 2$ keV). In the last observation, the Power-law index changes by $\delta\Gamma \sim 0.2$, maintaining the disk temperature around 0.63 keV (see Table 2). Perhaps the most important and main support for anti-correlated lag comes from the observed soft and hard X-ray flux values. It can be seen from Table 2 that as the soft flux increases, the corresponding hard flux decreases, and vice-versa. It suggests that the flux is an important parameter which changes during the lag. In the first two observations (see Table 2), the QPO centroid frequency is shifted during the lags, indicating that the size of the Compton cloud is altering. The soft flux is well correlated with the shift in the centroid frequency suggesting changes in the soft and hard emitting region in the accretion disk.

We have also investigated the dependence of the change in the QPO frequencies with the delays. In Figure 3, we have plotted the fractional change (in percentage) in the QPO frequency (absolute values) against the observed delays, for cases where the QPO frequencies were found to be decreasing. In Figure 4, a similar plot is shown for cases where the QPO frequencies were found to be increasing. Apart from the source H1743–322, we have used the data from Choudhury et al. (2005) for GRS 1915+105 and from Sriram et al. (2007) for the source XTE J1550–564. The fractional QPO frequency change (when the QPO centroid frequency is decreasing) in Figure 3 indicates that the disk radius is increasing (moving outwards), whereas in Figure 4, the fractional QPO frequency change (when the QPO centroid frequency is increasing) indicates that the disk radius is decreasing (moving inwards).

We attempt to give a qualitative description of these variations, based on some general considerations of a truncated accretion disk. First we take the case when the fractional change in QPO frequency is increasing as the delay period is increasing (Fig. 4). We assume that initially the disk is truncated at a large radius and then moves inward causing the soft flux to increase. The increase in the soft flux causes the hot corona to cool. If the observed QPO is linked to the size of the Compton cloud, an increase in the QPO frequency is expected.

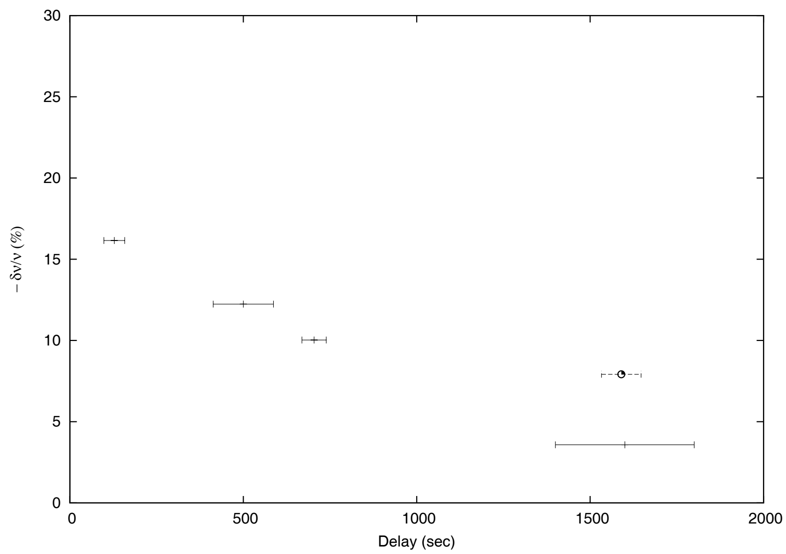

Fig. 3 Relation between the observed delay and the fractional percentile change (when QPO centroid frequency is decreasing) in the QPO frequency. The circle represents the data point of the second observation of the source H1743–322 and the remaining data points belong to the source GRS 1915+105.

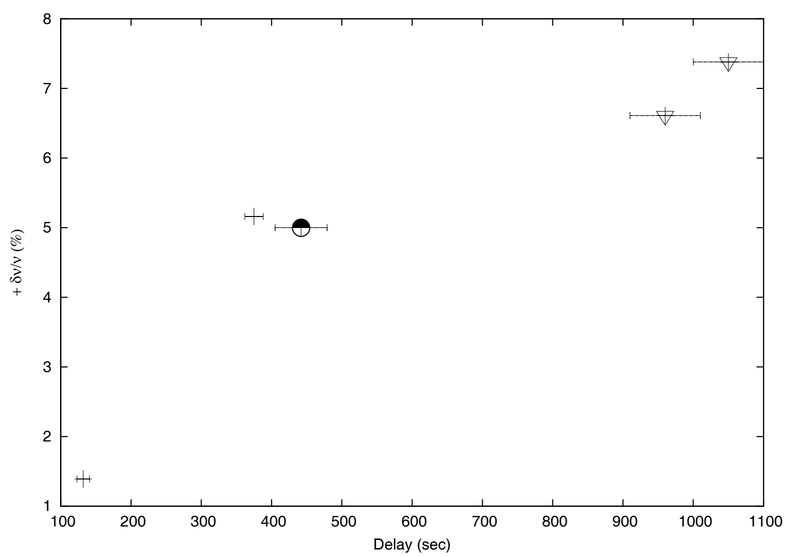

Fig. 4 Relation between the observed delay and the fractional percentile change (when QPO centroid frequency is increasing). The circle represents the data point of the first observation of the source H1743–322, the inverted triangle represents the data points of GRS 1915+105 and the remaining points are from XTE J1550–564.

The effective delay between two parts of the observation where positive change in the QPO frequency and pivoting in the spectra is observed can be given by

$$t_{\text{delay}} = t_{\text{viscous}} + |t_{\text{eff}}|, \tag{1}$$

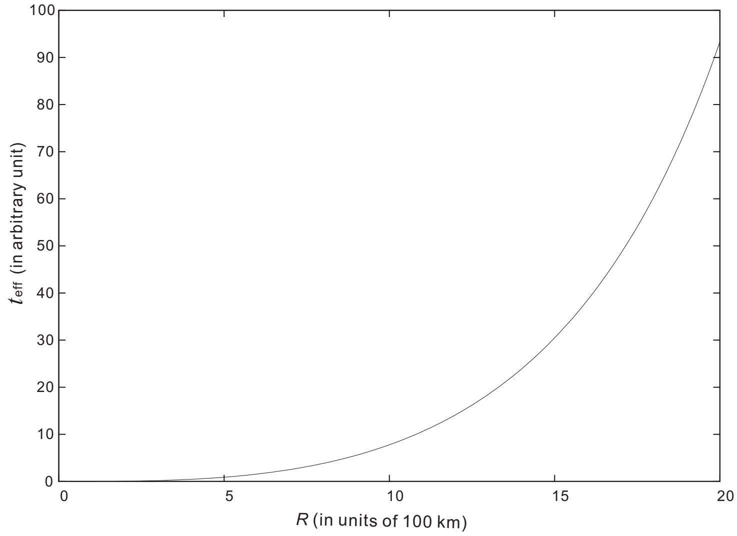

Fig. 5 Effective cooling/heating rate, $t_{\rm eff}$, for cooling (see text).

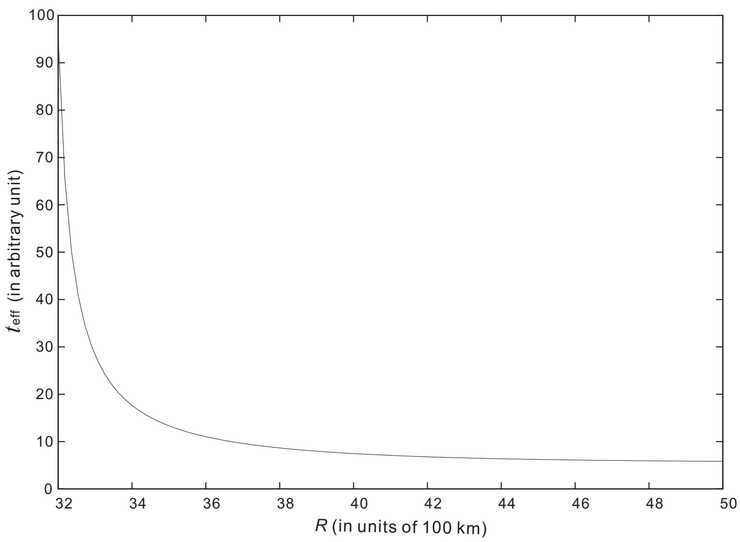

Fig. 6 Modulus of $t_{\rm eff}$ for heating (see text).

where $t_{\rm eff}$ is the effective cooling or heating time scale (will have positive values for cooling and negative values for heating). This time scale is given by

$$t_{\rm eff} = t_{\rm heat} \times t_{\rm cool}/(t_{\rm heat} - t_{\rm cool}), \quad (2)$$

$t_{\rm heat}$ is the heating time scale given by,

$$t_{\rm heat} = 10^{-3}\alpha^{-1} m_{10}^{-1/2} R_7^{3/2}, \quad (3)$$

where α is the dimensionless viscosity parameter, m_{10} is mass of the black hole expressed in terms of $m_{10} = M/10M_{\odot}$, R_7 is the size of the disk in terms of $R/(10^7\,{\rm cm})$ (see Frank et al. 2002).

t_{cool} is the cooling time scale given by,

$$t_{\mathrm{cool}} = \frac{N_{\mathrm{e}} kT}{\eta L_{\mathrm{seed}}}, \tag{4}$$

where N_{e} is the total number of electrons in the Compton cloud, η is the energy gain factor during Compton scattering and L_{seed} is the seed photon luminosity. Assuming that the seed photons are supplied by the standard thin accretion disk, the cooling time scale becomes

$$t_{\mathrm{cool}} = 10^{-6} \times R_7^3 \dot{M}_{17}^{-1} m_{10}^{-1} T_8, \tag{5}$$

where $\dot{M}_{17}$ is the mass accretion rate in terms of $\dot{M}/(10^{17}\ \mathrm{g\ s^{-1}})$, and T_8 is electron temperature in terms of $T/(10^8\ \mathrm{K})$.

For the present case (where the QPO frequency is increasing and the truncation radius is decreasing), the cooling is predominant. In Figure 5, we have plotted the effective cooling time scale as a function of radius. The delay is basically determined by the viscous time scale and hence will be large for a large truncation radius. Hence, if delay is high, then a small decrease in radius results in a large decrease in the cooling time scale causing the Compton cloud to shrink faster. This will give rise to a larger relative change in QPO frequency when the disk is truncated at a larger radius.

Now consider the other case where the negative change (decrease in QPO frequency) decreases with the delay (Fig. 3). Assume that initially the disk is truncated at a small radius and moves outward during the two different parts of an observation, causing the seed photon supply to the corona to decrease. Hence, we expect this will result in an effective heating of the corona and a decrease in QPO frequency. We plot the effective heating time scale as a function of truncation radius in Figure 6. In this figure we have taken the modulus of t_{eff} to make it positive. When the truncation radius (or delay) is small, a minute change in radius causes a large decrease in the effective heating time scale causing the corona to expand rapidly which in turn results in a large fractional decrease in QPO frequency. This scenario is evident in Figure 3.

To obtain the exact value of the truncation radius from the X-ray spectral fitting is quite difficult because we need to take into account the spectral hardening due to scattering, relativistic effects and other physical processes occurring very near to the black hole. However, the inner edge of the truncated accretion disk can act as a nozzle to launch the jet and the observed strong correlation of the X-ray and radio flux in Cyg X-3 and GRS 1915+105 (Choudhury et al. 2003), which are believed to be in the SPL state most of the time, may indicate the very significant role played by the truncated accretion disk.

In conclusion, the obtained results bias toward a truncated disk scenario favoring a *disk+sphere* geometry. Overall, the temporal and the spectral observations suggest that during the detected lag, the disk and Compton cloud emission property changes inversely and in this time span the disk is readjusted. The obtained lags are not state transition time scales but the scenario can be viewed as a mini state transition during which the properties of the soft and hard emitting region change.

Acknowledgements This research has made use of data obtained through HEASARC Online Service, provided by NASA/GSFC, in support of the NASA High Energy Astrophysics Programs. K.S is supported by UGC through the RFSMS scheme and is thankful to TIFR for providing the facility to carry out the work.

References

Abramowicz, M. A., & Kluzniak, W. 2001 A&A, 374, L19
Baba, D., Nagata, T., Iwata, I., Kato, T., & Yamaoka, H. 2003, IAU Circ., 8112
Belloni, T., et al. 2005, A&A, 440, 207
Chakrabarti, S. K., & Manickam, S. G. 2000, ApJ, 531, L41
Choudhury, M., Rao, A. R., Vadawale, S. V., & Jain, A. K. 2003, ApJ, 593, 452
Choudhury, M., & Rao, A. R. 2004, ApJ, 616, L143

Choudhury, M., Rao, A. R., Dasgupta, S., Pendharkar, J., Sriram, K., & Agrawal, V. K. 2005, ApJ, 631, 1072
Koerding, E., & Falcke, H. 2004, A&A, 414, 795
Corbel, S., Tomsick, J. A., & Kaaret, P. 2006, ApJ, 636, 971
Done, C., & Kubota, A. 2006, MNRAS, 371, 1216
Done, C., Gierliski, M., & Kubota, A. 2007, Ast. Ap. Rev, in press (astro-ph/0708.0148)
Doxsey, R., Bradt, H., Fabbiano, G., et al. 1977, IAUC 3113
Esin, A. A., McClintock, J. E., & Narayan, R. 1997, ApJ, 489, 865
Fender, R., Belloni, T., & Gallo, E. 2004 MNRAS, 355, 1105
Frank, J., King, A. R., & Raine, D. J. 2002, Accretion Power in Astrophysics (3rd ed.; Cambridge: Cambridge University Press), Chap. 5
Homan, J., Miller, J. M., Wijnands, R., et al. 2005, ApJ, 623, 383
Jahoda, K., et al. 2006, ApJS, 163, 401
Kalemci, E., Tomsick, J. A., Rothschild, R. E., Pottschmidt, K., Corbel, S., & Kaaret, P. 2006, ApJ, 639, 340
Kaluzienski, L. J., & Holt, S. S. 1977, IAU Circ., 3099
Kubota, A., & Makishima, K. 2004, ApJ, 601, 428
Lei, Y. J., et al. 2008, ApJ, 677, 461
Makishima, K., et al. 1986, ApJ, 308, 635
Markoff, S., Nowak, M. A., & Wilms, J. 2005, ApJ, 635, 1203
Markwardt, C. B., & Swank, J. H. 2003, The Astronomer's Telegram, 136
McClintock, J. E., & Remillard, R. A. 2004, in Compact Stellar X-ray Sources, eds., W. H. G. Lewin, & M. van der Klis (Cambridge: Cambridge University Press), astro-ph/0306213
McClintock, J. E., et al. 2007, astro-ph:0705.1034v1
Remillard, R. A., & McClintock, J. E. 2006, ARA&A, 44, 49
Remillard, R. A., McClintock, J. E., Orosz, J. A., & Levine, A. M. 2006, ApJ, 637, 1002
Revnivtsev, M., Chernyakova, M., Capitanio, F., et al. 2003, The Astronomer's Telegram, 132
Rodriguez, J., Corbel, S., Kalemci, E., Tomsick, J. A., & Tagger, M. 2004, ApJ, 612, 1018
Rothschild, R. E., et al. 1995, Proc. SPIE, 2518, 13
Rupen, M. P., Dhawan, V., & Mioduszewski, A. J. 2003, The Astronomer's Telegram, 210
Rupen, M. P., Mioduszewski, A. J., & Dhawan, V. 2004, Bulletin of the American Astronomical Society, 36, 937
Shapiro, S. L., Lightman, A. P., & Eardley, D. N. 1976, ApJ, 204, 187
Sriram, K., Agrawal, V. K., Pendharkar, Jayant K., & Rao, A. R. 2007, ApJ, 661, 1055
Steeghs, D., Miller, J. M., Kaplan, D., & Rupen, M. 2003, The Astronomer's Telegram, 146
Sunyaev, R. A., & Titarchuk, L. G. 1980, A&A, 86, 121
Titarchuk. L., & Fioroti, R. 2004, ApJ, 612, 988
Tomsick, J., Corbel, S., Goldwurm, A., & Kaaret, P. 2005, ApJ, 630, 413
Zdziarski, A. A., Johnson, W. N., & Magdziara, P. 1996, MNRAS, 283, 193
Zdziarski, A. A., Poutanen, J., Paciesas, W. A., et al. 2002, ApJ, 578, 357
Zdziarski, A. A., & Gierliski, M. 2004, Progress of Theoretical Physics Supplement, 155, 99